Electronic Supplementary Material (ESI) for Physical Chemistry Chemical Physics.

SUPPORTING INFORMATION

Mechanistic Investigations of the 2-Coumaranone Chemiluminescence

Stefan Schramm[1,3*], Isabelle Navizet[2], Pascal Oesau[3], Durga Prasad Karothu[1], Veronika Bensmann[3], Dieter Weiss[3], Rainer Beckert[3], Panče Naumov[1]

[1]*New York University Abu Dhabi, P. O. Box 129188, Abu Dhabi, United Arab Emirates*

[2]*Université Paris-Est, Laboratoire Modélisation et Simulation Multi Echelle, MSME UMR 8208 CNRS, 5 bd Descartes, 77454 Marne-la-Vallée, France*

[3]*Friedrich-Schiller-Universität Jena, Institut für Organische Chemie und Makromolekulare Chemie, Humboldtstr. 10, 07743 Jena, Germany*

Email: stefan.schramm@uni-jena.de

Contents

1. Computational Details

Density Functional Theory (DFT) and time-dependent Density Functional Theory (TD-DFT) calculations were done with Gaussian G09 program package [S1] and visualized with GaussView5 [S2]. The ground state geometries and first excited state optimized geometries were obtained at the DFT and TD-DFT B3LYP/6-31+G(d,p) [S3] level of theory. The calculations were done with implicit solvent, by using the polarizable continuum model (PCM) [S4] with the standard parameters of G09 for acetonitrile (MeCN). Emission wavelengths were calculated with Linear-Response. The Linear Response emission energies were sufficient and the more computationally demanding none equilibrium state-specific PCM (SS) were deemed unnecessary [S5] for calculation of the emission energies. In earlier studies [S16] we have already compared this method for the 2-coumaranones against other computational methods and found it give for this particular system similar accuracies than CASSCF and CASPT2 calculation with large active spaces. The typical error of CASPT2 calculations on Dioxetanones are <1 kcal mol^{-1}. [S17] The IBO calculations and analysis were done using IBOview v20150427 [S6], and the Mulliken and NBO population analysis were applied as implemented in the Gaussian G09 program package.

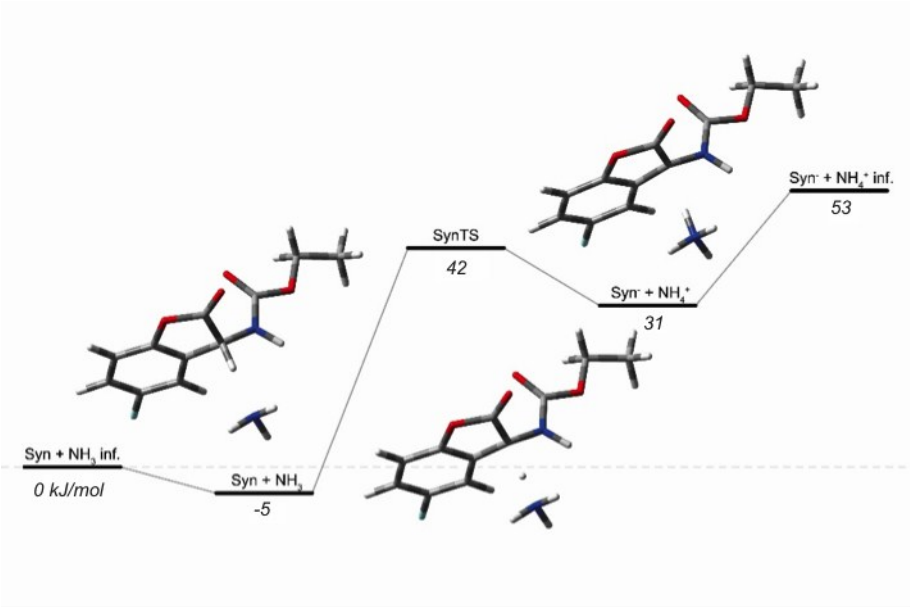

Figure S1. Potential energy diagram for deprotonation of the *syn*-conformer of the 2-coumaranone with ammonia as model base. The B3LYP/6-31+G(d,p)-calculated energies in MeCN (PCM) are given in kJ mol^{-1}

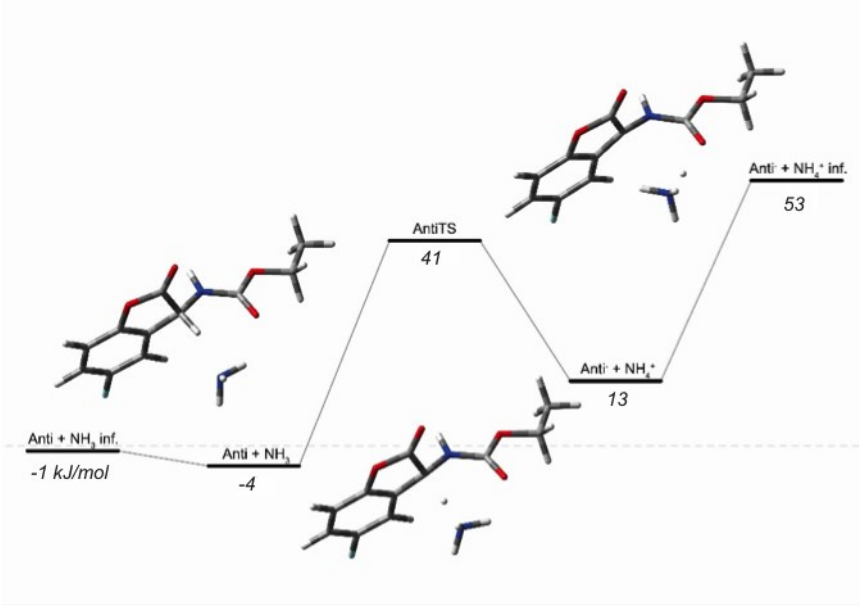

Figure S2. Potential energy diagram for deprotonation of the *anti*-conformer of the 2-coumaranone with ammonia as model base. The B3LYP/6-31+G(d,p)-calculated energies in MeCN (PCM) are given in kJ mol^{-1}

Table S1. B3LYP[S5]/6-31+G(d,p) in MeCN relative energies (in kcal mol^{-1}) of optimized structures corresponding of the compound **2** (**2c**, **2n** and **2o**)

	relative energy (kJ mol^{-1})
2n (from *syn* compound 1)	58.8
2n (from *anti* compound 1)	57.3
2o	61.8
2c	0.0

Table S2. Population Analysis (Mulliken and IBO) the Peroxyanion-O, the Lacton-C, and the Carbamate-C of the peroxyanion **(6)** and the deprotonated 2-coumaranone **(2c)**

6	**Mulliken**	**IBO**
Peroxyanion-O_{18}	-0.750	-0.631
Lacton-C_9	0.884	0.458
Carbamate-C_{13}	0.634	0.549

2c	**IBO**
Lacton-O_{18}	-0.55
Lacton-C_9	0.40
Deprot-C_{10}	-0.13

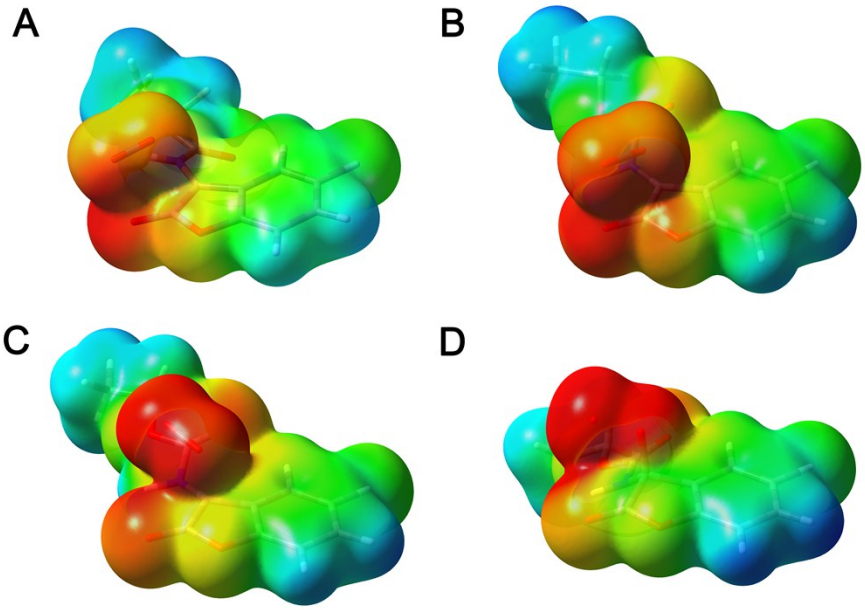

Figure S3: Electrostatic potential (Isovalues: Red: -0.230, Blue: 0.01) mapped on the surface of the total electron density (Isovalue 0.004) for the approach of molecular oxygen towards **2** at a distance of C10-O18 of A: 3.0 Å, B: 2.8 Å, C: 2.2 Å, D: 1.4 Å

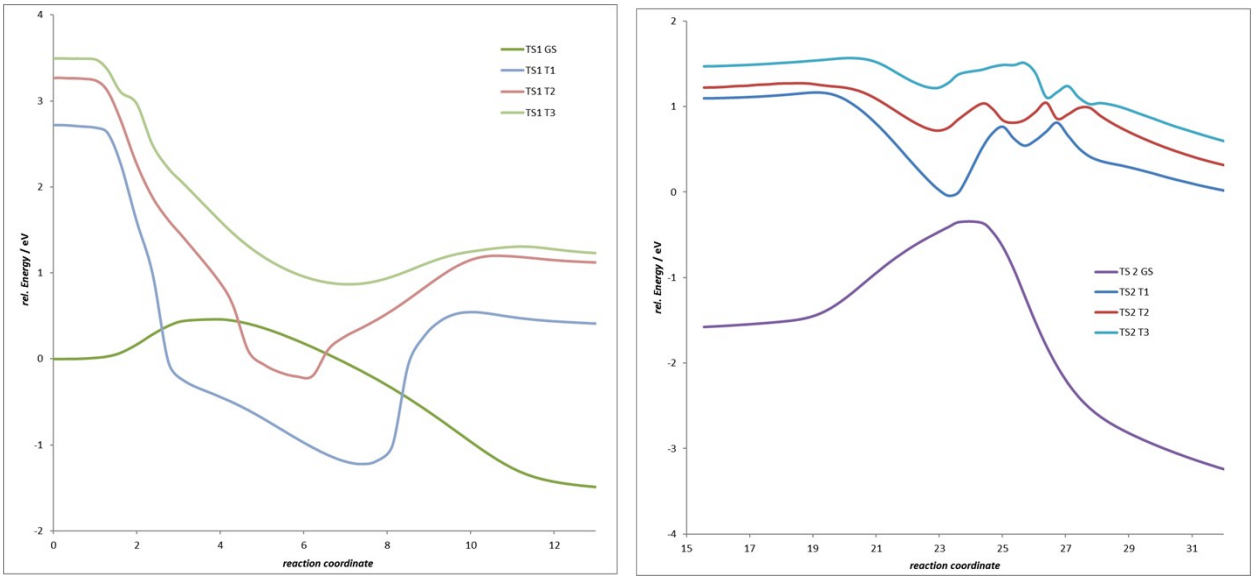

Figure S4: Internal Reaction Coordinate (IRC) of the decomposition of the 1,2-dioxetanone 3 with triplet excitation. Similar to the data resulted from singlet excitations, conical intersections can be proposed near to both involved transition states.

2. Single crystal X-ray diffraction

The diffraction data for compound **1** were collected on a Bruker APEX DUO diffractometer with a graphite monochromator, Cu*K*α radiation (λ = 1.54178 Å) and CCD as area detector [S7]. All crystallographic calculations were performed using the crystallographic software APEX 2 [S7]. The data were scaled and absorption correction was performed using SADABS [S8]. The structure of compound **(1)** was solved by direct methods using SHELXS97 [S9] and refined by full-matrix least-squares methods based on F^2 using SHELXL97 [S9] which are embedded in the suite WinGX [S10]. The non-hydrogen atoms were anisotropically refined [S11]. The hydrogen atoms attached to nitrogen atom was located from the difference electron density map and refined with isotropic thermal parameters. All hydrogen atoms attached to carbon were fixed geometrically using the HFIX command in SHELX-TL [S9]. Crystallographic data for the structure of **1** were deposited in the Cambridge Crystallographic Data Center (deposition No. CCDC 1519439).

The packing diagrams were generated using Mercury 3.7 [S12] and X-Seed [S13], and the images were rendered with POV-Ray [S14].

Table S3. Crystallographic details of compound 1

Temperature / K	100 K
Formula weight	239.2
Crystal system	Triclinic
Space group	$P\bar{1}$
a / Å	5.0027(3)
b / Å	9.6906(6)
c / Å	10.9373(6)
α / º	95.710(2)
β / º	98.317(2)
γ / º	93.853(2)
Volume / Å^3	520.26(2)
Z	2
Density / (g cm^{-3})	1.53
μ / mm^{-1}	1.108
F_{000}	248.0
$h_{min,}$ h_{max}	-5, 5
$k_{min,}$ k_{max}	-11, 11
$l_{min,}$ l_{max}	-13, 13
No. of measured reflections	13554
No. of unique reflections	1777
No. of reflections used	1689
R_{all}, R_{obs}	0.033, 0.032
$wR_{2,all}$, $wR_{2,obs}$	0.083, 0.082

$\Delta\rho_{min,max}$ / (e Å^{-3})	-0.232, 0.294
GooF	1.042
CCDC No:	1519439

The crystal structure of **1** was determined from colorless, needle-shaped crystals obtained from a 9:1 mixture of acetone and water (the crystallographic details are provided in Table S3, Supporting Information). In the structure, the molecules interact via hydrogen bonds N—H···O (Figure 1) in the direction close to the crystallographic *b* axis, with *d*(N12···O11) = 3.074(2) Å and *d*(H12···O11) = 2.216(3) Å. The packing is stabilized by weak intermolecular interactions C—H···F (*d*(C16···F7) = 3.360(2) Å, *d*(H16···F7) = 2.588(2) Å, Figure S3, Supporting Information).

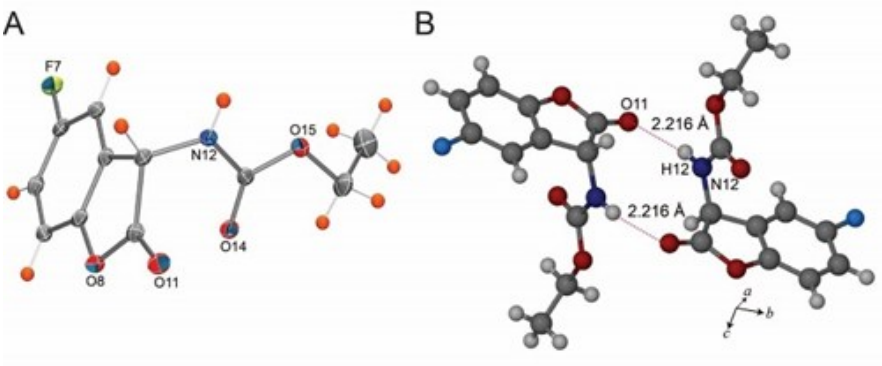

Figure S5. Molecular structure and hydrogen bonding in the crystal of **1**. (A) ORTEP of the molecular structure drawn at 50% ellipsoid probability. (B) Hydrogen bonds between two molecules (represented by broken lines).

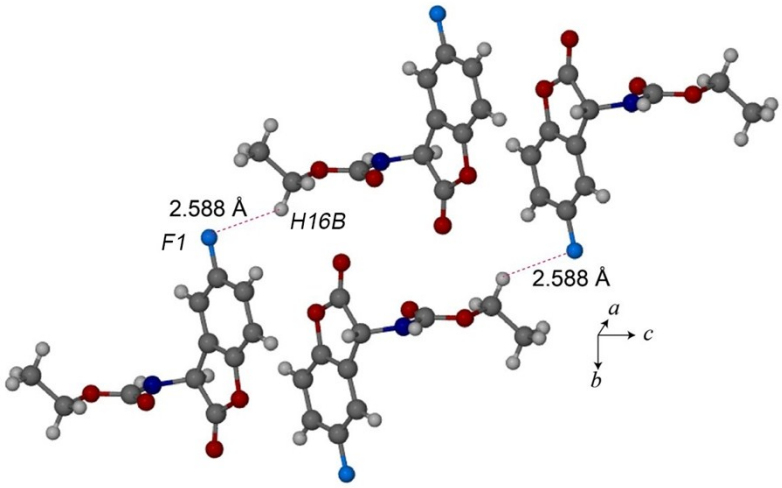

Figure S6. The crystal packing of compound **1** shows C–H···F intermolecular interactions along crystallographic *c* axis.

Table S4. Atomic coordinates (Å x 10^4) and equivalent isotropic displacement parameters (Å^2 x 10^3) for compound **1**. U(eq) is defined as one third of the trace of the orthogonalized U^{ij} tensor.

	x	y	z	U(eq)
C1	5828(3)	9653(1)	1992(1)	16(1)
C2	4021(3)	10567(1)	2368(1)	17(1)
C3	2544(3)	10253(1)	3306(1)	17(1)
C4	3018(3)	9030(1)	3811(1)	15(1)
C5	4847(3)	8127(1)	3439(1)	14(1)
C6	6311(3)	8426(1)	2504(1)	15(1)
F7	7230.0(1)	9986(8)	1072(7)	21(1)
O8	1683(2)	8550(9)	4748(8)	16(1)
C9	2588(3)	7286(1)	4994(1)	15(1)
C10	4834(3)	6931(1)	4221(1)	14(1)
O11	1691(2)	6644(9)	5745(8)	19(1)
N12	4340(2)	5544(1)	3572(1)	15(1)
C13	1912(3)	5180(1)	2859(1)	14(1)
O14	8(2)	5900(9)	2848(8)	17(1)
O15	1907(2)	3947(1)	2175(9)	20(1)
C16	-658(3)	3387(1)	1427(1)	24(1)
C17	-157(4)	2909(1)	143(1)	32(1)

Table S5. Bond lengths [Å] and angles [°] for compound **1**

F(7)-C(1)	**1.359(1)**
O(8)-C(9)	1.371(2)
O(8)-C(4)	1.401(1)
O(11)-C(9)	1.197(2)
O(14)-C(13)	1.217(2)

O(15)-C(13)	1.345(2)
O(15)-C(16)	1.458(2)
N(12)-H(12)#1	0.880
N(12)-C(10)#1	1.445(2)
N(12)-C(13)	1.350(2)
C(10)-H(10)	1.000
C(10)-C(9)	1.538(2)
C(10)-C(5)	1.507(2)
C(5)-C(4)	1.383(2)
C(5)-C(6)	1.383(2)
C(1)-C(6)	1.385(2)
C(1)-C(2)	1.382(2)
C(4)-C(3)	1.377(2)
C(3)-H(3)	0.950
C(3)-C(2)	1.393(1)
C(6)-H(6)	0.950
C(2)-H(2)	0.950
C(16)-H(16A)	0.990
C(16)-H(16B)	0.990
C(16)-C(17)	1.496(2)
C(17)-H(17A)	0.980
C(17)-H(17B)	0.980
C(17)-H(17C)	0.980
C(9)-O(8)-C(4)	108.2(9)
C(13)-O(15)-C(16)	116.8(1)
C(10)-N(12)-H(12)#1	120.8
C(13)-N(12)-H(12)#1	120.8
C(13)-N(12)-C(10)#1	118.5(1)
N(12)-C(10)-H(10)#1	108.7
N(12)-C(10)-C(9)#1	111.9(1)
N(12)-C(10)-C(5)#1	117.1(1)
C(9)-C(10)-H(10)	108.7
C(5)-C(10)-H(10)	108.7

C(5)-C(10)-C(9)	101.2(1)
O(14)-C(13)-O(15)	125.5(1)
O(14)-C(13)-N(12)	123.2(1)
O(15)-C(13)-N(12)	111.3(1)
O(8)-C(9)-C(10)	110.0(1)
O(11)-C(9)-O(8)	120.9(1)
O(11)-C(9)-C(10)	129.0(1)
C(4)-C(5)-C(10)	108.0(1)
C(4)-C(5)-C(6)	120.1(1)
C(6)-C(5)-C(10)	131.9(1)
F(7)-C(1)-C(6)	118.1(1)
F(7)-C(1)-C(2)	118.0(1)
C(2)-C(1)-C(6)	123.9(1)
C(5)-C(4)-O(8)	112.3(1)
C(3)-C(4)-O(8)	123.9(1)
C(3)-C(4)-C(5)	123.8(1)
C(4)-C(3)-H(3)	121.7
C(4)-C(3)-C(2)	116.5(1)
C(2)-C(3)-H(3)	121.7
C(5)-C(6)-C(1)	116.2(1)
C(5)-C(6)-H(6)	121.9
C(1)-C(6)-H(6)	121.9
C(1)-C(2)-C(3)	119.5(1)
C(1)-C(2)-H(2)	120.3
C(3)-C(2)-H(2)	120.3
O(15)-C(16)-H(16A)	109.9
O(15)-C(16)-H(16B)	109.9
O(15)-C(16)-C(17)	108.8(1)
H(16A)-C(16)-H(16B)	108.3
C(17)-C(16)-H(16A)	109.9
C(17)-C(16)-H(16B)	109.9
C(16)-C(17)-H(17A)	109.5
C(16)-C(17)-H(17B)	109.5

C(16)-C(17)-H(17C)	109.5
H(17A)-C(17)-H(17B)	109.5
H(17A)-C(17)-H(17C)	109.5
H(17B)-C(17)-H(17C)	109.5

3. Experimental details

3.1. NMR spectroscopy

In order to get an experimental insight into the deprotonation reaction of the 2-coumaranone **1**, 10 mg of it were dissolved in about 0.3 mL of methanol-d_4 and treated with 0.2 mL D_2O. One-dimensional proton NMR spectrum was recorded using a BRUKER AC 400 NMR spectrometer.

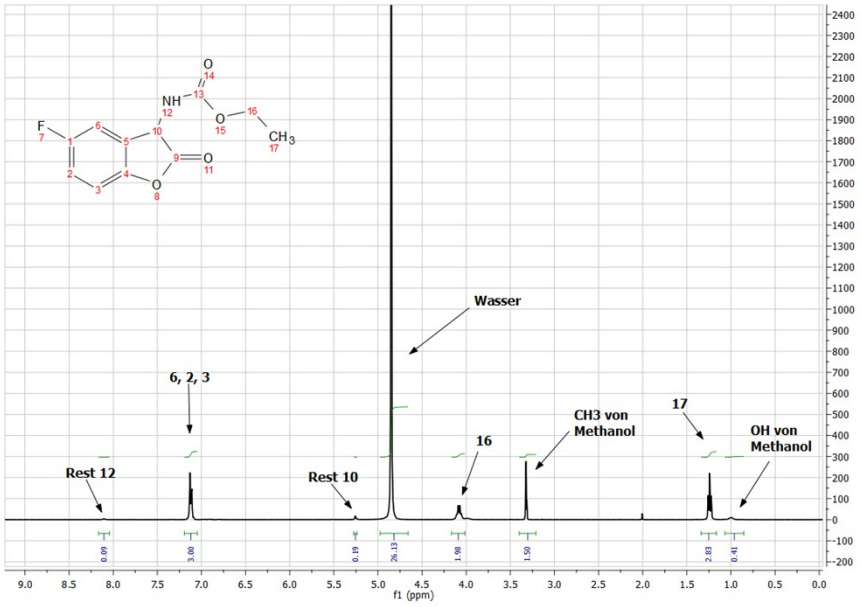

Figure S7. ^{1}H NMR deuterium exchange spectrum of compound **1** in deuterated H_2O/MeOH

3.2. In situ singlet O_2 generation experiment

To further investigate the reactions of a potential enolate, singlet oxygen was required to be generated in situ. For doing this the photosensitizer Bengal Rose B was added to a 10^{-5} M solution of the tested coumaranone in MeCN so that its maximum absorbance was less than 1. The test solution was then excited for 5 min at the maximum wavelength of absorbance of the Bengal Rose B using a JASCO FP6500 spectrofluorimeter, and the excitation light was maintained during the rest of the experiment. The chemiluminescence of the 2-coumaranone was initiated by addition of a 100-fold excess of the base DBU (1,8-diazabicyclo[5.4.0]undec-7-en) and the light decay with time was followed at the wavelength of maximum emission (ca. 430 nm) until no light could be observed. As a reference, the reaction without the excitation of Bengal Rose B carried out. Moreover, the following negative controls were carried out: a) absence of coumaranone, b) absence of Bengal Rose B, c) absence of coumaranone, absence of Bengal Rose, d) absence of coumaranone, no excitation, e) absence of Bengal Rose, no excitation, and f) absence of coumaranone, absence of Bengal Rose, no excitation.

Table S6. Quotient of the first order kinetic rate constant and the CL quantum yields for the reaction with singlet oxygen (SO) and triplet oxygen (TO) and three different 2-coumaranones **(1, 1b, 1c)**

	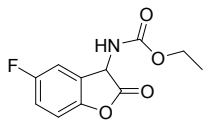	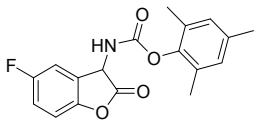	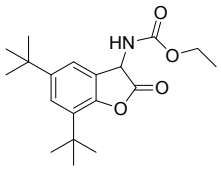
	(1)	**(1b)**	**(1c)**
$k_{SO/TO}$	1.47±0.02	1.89±0.04	1.05±0.07
$\Phi_{CL\ SO/TO}$	7.14±0.41	10.03±0.26	4.24±0.15

3.3. SET EPR spectroscopy

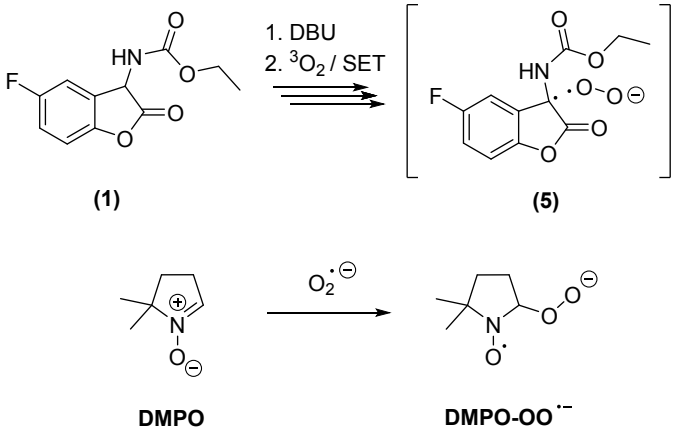

Figure S8. Single electron transfer of coumaranone **1** and the reaction of DMPO with superoxide radical anions

In order to get a closer insight into the electron-transfer reaction of the deprotonated form of the 2-coumaranone **1**, we used EPR spectroscopy with the spin-trapping reagent DMPO (5,5-dimethyl-1-pyrroline N-oxide). DMPO is well known for its ability to form metastable adducts with superoxide radical anions that can be detected via ESR spectroscopy due to their odd spin number. The reactions conditions as described in literature were used [S15] with acetonitrile as solvent and the spectra were recorded with BRUKER X-band EPR spectrometer. The reaction was initiated by catalytic amounts of DBU. As a negative control and to exclude OH-radicals the same reaction was carried out without the use of 2-coumaranone. The resulting spectra were found to be in agreement to the literature on DMPO-OO adducts. Therefore, we conclude the DMPO-OO adduct was present in the conducted experiments and consequently that the mechanism of the 2-Coumaranone chemiluminescence has to include a single electron transfer leading to superoxide radical anions.

4. Coordinates

Coordinates of atoms of the different optimized compounds in the pathway from the 2-coumaranone to the emitter. Calculations were performed with Gaussian G09, with the options B3LYP[S5]/6-31+G(d,p), and MeCN (PCM) as solvent.

Compound 1:

H	-0.42697000	2.07320700	-0.84230600
C	-0.62391600	1.94206700	0.21599300
C	-1.14794500	1.67193900	3.00773200
C	-0.65563700	0.69105000	0.82220900
C	-0.85755600	3.03969900	1.04189500
C	-1.11853400	2.93731500	2.40521100
C	-0.91065200	0.58321600	2.18623300
H	-1.29280600	3.83507500	2.98754800
H	-1.34279900	1.55596200	4.06754800
F	-0.83137300	4.28433000	0.48178300
C	-0.49191400	-0.70325700	0.27161800
H	-1.35205400	-0.98951400	-0.34691600
C	-0.57387700	-1.55573600	1.56443200
O	-0.88484600	-0.74393600	2.62726100
O	-0.41350200	-2.74200100	1.69282500
N	0.68439500	-0.96302800	-0.51394000
H	1.59636800	-0.72167700	-0.14884500
C	0.61791900	-1.57826700	-1.73247300
O	1.85246600	-1.72885500	-2.24949900
C	1.93829700	-2.36189200	-3.55794100
H	1.36140400	-1.76478800	-4.26918500
H	1.48845100	-3.35600900	-3.49078700
O	-0.42062500	-1.93375100	-2.27942300
C	3.40485100	-2.42810900	-3.93377500
H	3.97109100	-3.02175500	-3.20984200
H	3.50281600	-2.90015300	-4.91635000
H	3.84343900	-1.42720100	-3.98868300

Compound 2c:

H	-0.70560000	-2.08300000	0.78440000
C	-1.44740000	-1.41210000	0.36400000
C	-3.47430000	0.27580000	-0.73130000
C	-1.13090000	-0.10990000	-0.06290000
C	-2.77120000	-1.81780000	0.22440000
C	-3.79040000	-1.03070000	-0.30300000
C	-2.16570000	0.69780000	-0.60080000
H	-4.79860000	-1.42170000	-0.37880000
H	-4.23730000	0.92540000	-1.14870000
F	-3.09520000	-3.09350000	0.63940000
C	0.05000000	0.69060000	-0.10390000
C	-0.27170000	1.94600000	-0.65240000
O	-1.67160000	1.93040000	-0.95870000
O	0.36970000	2.98340000	-0.89900000
N	1.34070000	0.32910000	0.34740000
H	1.62700000	0.54690000	1.29480000
C	2.28100000	-0.27540000	-0.43020000
O	3.42180000	-0.47480000	0.28280000
C	4.51790000	-1.12010000	-0.41240000
H	4.77880000	-0.52200000	-1.29030000
H	4.18710000	-2.10560000	-0.75340000
O	2.14590000	-0.60810000	-1.60440000
C	5.67730000	-1.22400000	0.56000000
H	6.52410000	-1.70900000	0.06400000
H	5.99860000	-0.23370000	0.89730000
H	5.40510000	-1.82120000	1.43580000

Compound 3:

C	-0.79839300	-0.69270800	4.18943100
C	0.27887400	-1.57787500	4.24944000
C	0.96833300	-1.86390500	3.08187200
C	0.62163600	-1.29515900	1.81292500
C	-0.49065000	-0.37302100	1.81365800
C	-1.18615100	-0.09768900	3.00975000
F	-1.49302900	-0.40837800	5.34639400
O	1.29247400	-1.62042700	0.74446000
C	-1.51274100	1.74109500	0.71946200
C	-0.96753600	0.30273500	0.55821400
O	-2.81660100	1.39230100	0.53488600
N	-0.13220100	0.04038700	-0.53298200
C	-0.22149500	0.71190600	-1.71852900
O	-1.01484200	1.61679000	-1.96083000
O	0.69125300	0.24276400	-2.59249400
C	0.72597600	0.87535500	-3.90130900
C	1.79625500	0.17603200	-4.71568600
O	-2.45853300	-0.03193700	0.27760000
O	-1.09192600	2.82776100	1.00079900
H	0.56115200	-2.02856700	5.19627000
H	1.80740900	-2.55339700	3.10000300
H	-2.03898800	0.57459700	3.01866500
H	0.60307100	-0.69383700	-0.31623200
H	-0.26219000	0.77996700	-4.35955100
H	0.94594300	1.93824700	-3.76755300
H	1.84745800	0.63139500	-5.70968400
H	2.77807900	0.27292700	-4.24256100
H	1.56756200	-0.88716000	-4.83651700

Compound 4:

C	0.46286100	4.38408700	-0.18566100
C	-0.92934300	4.40754700	-0.32913000
C	-1.62011200	3.20821600	-0.33695200
C	-0.96545500	1.93698800	-0.20387800
C	0.47545300	1.97326400	-0.05954600
C	1.16129600	3.20910200	-0.05335200
F	1.14412600	5.58545700	-0.17875000
C	1.30859400	0.75658700	0.08741800
O	-1.65785200	0.83916600	-0.21621300
O	2.53863300	0.78822100	0.21407300
N	0.56577500	-0.42225600	0.07026800
C	1.02794400	-1.71300100	0.17585600
O	2.18409700	-2.09139300	0.28981500
O	-0.03566100	-2.55566300	0.13208100
C	0.25629800	-3.97382400	0.23241000
C	-1.06423400	-4.71652500	0.17074700
H	-1.44749300	5.35667100	-0.43182300
H	-2.70086100	3.20186400	-0.44655500
H	2.24040100	3.21388000	0.05659400
H	-0.46522700	-0.23847200	-0.03886000
H	0.91912600	-4.25376100	-0.59147300
H	0.78129200	-4.15676900	1.17444200
H	-0.87760600	-5.79249400	0.24574500
H	-1.71989900	-4.42369000	0.99645400
H	-1.58205400	-4.52320200	-0.77370900

Compound 6:

H	0.69911600	-1.99745800	0.76124800
C	1.48892200	-1.38774100	0.34250300
C	3.59424100	0.18389100	-0.76042000
C	1.28902700	-0.04452100	0.03581900
C	2.75029500	-1.91237500	0.07020400
C	3.79773400	-1.17160300	-0.46638600
C	2.33884900	0.70266900	-0.49503000
H	4.75532400	-1.64530000	-0.65162200
H	4.38544400	0.79659200	-1.17688300
F	2.97097800	-3.23352600	0.34836200
C	0.12309200	0.89631500	0.26898100
C	0.65060300	2.17925900	-0.45518700
O	1.98690200	2.03027000	-0.73957900
O	0.05787900	3.19015700	-0.73372600
N	-1.14934600	0.58377700	-0.35547500
H	-1.67349200	1.40586500	-0.63340700
C	-1.92890400	-0.48522000	0.00252700
O	-3.19039400	-0.30268900	-0.45068300
C	-4.12874200	-1.38819300	-0.22075900
H	-4.20842800	-1.55741400	0.85657200
H	-3.73199900	-2.29497600	-0.68603100
O	-1.55360900	-1.48338400	0.60391500
C	-5.45606800	-0.97768600	-0.82737100
H	-6.18630000	-1.77825600	-0.67278800
H	-5.83992700	-0.06742100	-0.35690200
H	-5.36040400	-0.80360200	-1.90347900
O	0.07083900	1.11343100	1.65823800
O	-0.95071300	2.12071200	2.00033000

Compound 7:

H	0.47924700	-2.10549600	0.48383000
C	1.29329100	-1.45637400	0.18534300
C	3.45397700	0.21807500	-0.58632200
C	1.12567000	-0.07584700	0.08947500
C	2.55351900	-1.96471600	-0.11071900
C	3.62872300	-1.16786100	-0.48773900
C	2.19783400	0.75134700	-0.29324700
H	4.58869300	-1.62506200	-0.70324700
H	4.27428600	0.86141000	-0.88566800
F	2.74716300	-3.32189300	-0.02026700
C	-0.04665900	0.82090000	0.35114200
C	0.43857200	2.26496400	-0.06703800
O	1.90233300	2.07559600	-0.38146700
O	-0.16177600	3.03220300	-0.85540700
N	-1.31531300	0.53025500	-0.22324300
H	-1.73973200	1.31431800	-0.71340100
C	-2.10842200	-0.52716500	0.11576500
O	-3.31598600	-0.41778900	-0.47924300
C	-4.26920700	-1.48357300	-0.21619400
H	-4.43139500	-1.54609900	0.86331000
H	-3.83687300	-2.42813800	-0.55763100
O	-1.77824900	-1.45474200	0.84739000
C	-5.54575800	-1.14529000	-0.96034200
H	-6.28587600	-1.93168100	-0.78202200
H	-5.96387400	-0.19539100	-0.61368700
H	-5.36818000	-1.07889000	-2.03799300
O	-0.10098600	1.24368600	1.74461100
O	0.36852200	2.62861200	1.41199100

Compound 8:

C	-3.67965100	-0.15227300	0.08443200
C	-3.72849600	-1.59259600	0.20095200
C	-2.59461400	-2.32400200	0.10013400
C	-1.30434100	-1.69365600	-0.16510600
C	-1.27754200	-0.17052000	-0.33365500
C	-2.55807700	0.54746700	-0.13738900
F	-4.88026300	0.47676700	0.20008000
O	-0.27884800	-2.38007100	-0.25836700
C	0.01547400	2.03876300	0.38123500
C	0.03815300	0.58221700	-0.19374400
O	-0.05705600	2.97602700	-0.44555800
N	1.19818800	-0.17818700	0.10276700
C	2.47786900	0.29886100	0.01644700
O	2.82042700	1.46986300	-0.07035500
O	3.34004200	-0.74589000	0.06378700
C	4.75344000	-0.41932800	0.11268800
C	5.52065700	-1.72633100	0.15295000
O	-0.52203000	0.33035500	-1.48298200
O	0.04353700	2.08106700	1.63647900
H	-4.69377400	-2.05973600	0.36948200
H	-2.60169900	-3.40554700	0.17746600
H	-2.57214500	1.62579400	-0.24401400
H	1.08340800	-1.18666900	0.00452500
H	5.00774800	0.17483600	-0.76924500
H	4.93855800	0.18712600	1.00412400
H	6.59313700	-1.51384500	0.20451700
H	5.24541400	-2.31810300	1.03130400
H	5.33152200	-2.32199300	-0.74529600

References:

[S1] Frisch, M. J. T., G. W.; Schlegel, H. B.; Scuseria, G. E.; Robb, M. A.; Cheeseman, J. R.; Scalmani, G.; Barone, V.; Mennucci, B.; Petersson, G. A.; Nakatsuji, H.; Caricato, M.; Li, X.; Hratchian, H. P.; Izmaylov, A. F.; Bloino, J.; Zheng, G.; Sonnenberg, J. L.; Hada, M.; Ehara, M.; Toyota, K.; Fukuda, R.; Hasegawa, J.; Ishida, M.; Nakajima, T.; Honda, Y.; Kitao, O.; Nakai, H.; Vreven, T.; Montgomery, J., J. A.; Peralta, J. E.; Ogliaro, F.; Bearpark, M.; Heyd, J. J.; Brothers, E.; Kudin, K. N.; Staroverov, V. N.; Kobayashi, R.; Normand, J.; Raghavachari, K.; Rendell, A.; Burant, J. C.; Iyengar, S. S.; Tomasi, J.; Cossi, M.; Rega, N.; Millam, N. J.; Klene, M.; Knox, J. E.; Cross, J. B.; Bakken, V.; Adamo, C.; Jaramillo, J.; Gomperts, R.; Stratmann, R. E.; Yazyev, O.; Austin, A. J.; Cammi, R.; Pomelli, C.; Ochterski, J. W.; Martin, R. L.; Morokuma, K.; Zakrzewski, V. G.; Voth, G. A.; Salvador, P.; Dannenberg, J. J.; Dapprich, S.; Daniels, A. D.; Farkas, Ö.; Foresman, J. B.; Ortiz, J. V.; Cioslowski, J.; Fox, D. J.; Gaussian, Inc: Wallingford C, **2009**

[S2] GaussView, **Version 5**, Roy Dennington, Todd Keith, and John Millam, *Semichem Inc*., Shawnee Mission, KS, **2009**.

[S3] (a) Becke AD. Density-functional thermochemistry. III. The role of exact exchange. *J Chem Phys* **1993**, 98:5648e52. (b) Lee C, Yang W, Parr RG. Development of the Colle-Salvetti correlation- energy formula into a functional of the electron density. *Phys Rev B* **1993**, 37:785e9.

[S4] (a) Cances E, Menucci B, Tomasi J. A new integral equation formalism for the polarizable continuum model: theoretical background and applications to isotropic and anisotropic dielectrics. *J Chem Phys* **1997**, 107:3032e41. (b) Menucci B, Cances E, Tomasi J. Evaluation of solvent effects in isotropic and anisotropic dielectrics and in ionic solutions with a unified integral equation method: theoretical bases, computational implementation, and numerical applications. *J Phys Chem B* **1997**, 101:10506e17.

[S5] (a) Improta, R; Barone, V.; Scalmani, G.; Frisch, M. J. *J. Chem. Phys.* **2006**, *125*, 054103. (b) Improta, R; Scalmani, G.; Frisch, M. J.; Barone, V. J. *Chem. Phys.* **2007**, *127*, 074504.

[S6] a) G. Knizia, J. Chem. Theory Comput., **2013**, *9*, 4834. b) G. Knizia, J.E.M.N. Klein, Angew. Chem. Int. Ed., **2015**, *54*, 5518.

[S7] APEX DUO, version 2.1-4, and SAINT, version 7.34A; Bruker AXS Inc.: Madison, WI, 2012.

[S8] Sheldrick, G. M. SADABS; University of Göttingen, Göttingen, Germany, 1996.

[S9] Sheldrick, G. M. *Acta Crystallogr.* A **2008**, *64*, 112–122.

[S10] Farrugia, L. *J. Appl. Cryst.* **1999**, *32*, 837–838.

[S11] Sheldrick, G. M. SHELXL-97; University of Göttingen: Göttingen, Germany, 2008.

[S12] Macrae, C. F.; Bruno, I. J.; Chisholm, J. A.; Edgington, P. R.; McCabe, P.; Pidcock, E.; Rodriguez-Monge, L.; Taylor, R.; Streek, J. V.; Wood, P. A. *J. Appl. Cryst.* **2008**, *41*, 466–470.

[S13] L. J. Barbour, X-Seed, Graphical Interface to SHELX-97 and POV-Ray, Program for Better Quality of Crystallographic Figures, University of Missouri-Columbia, Columbus, MO, 1999

[S14] POV-RAY for Windows. 2004, Persistence of Vision, Raytracer Pty Ltd, Victoria, Australia.

[S15] B. R. Branchini, C. E. Behney, T. L. Southworth, D. M. Fontaine, A. M. Gulick, D. J. Vinyard, G. W. Brudvig, *Journal of the American Chemical Society*, **2015**, *137*, 7592-7595.

[S16] S. Schramm, I. Navizet, P. Naumov, N. K. Nath, R. Berraud-Pache, P. Oesau, D. Weiss, R. Beckert, *European Journal of Organic Chemistry* **2016**, *2016*, 678-681.

[S17] Farahani, P.; Baader, W. J. *The Journal of Physical Chemistry A* **2017**.